Journal of Zhejiang University-SCIENCE A (Applied Physics & Engineering)
ISSN 1673-565X (Print); ISSN 1862-1775 (Online)
www.zju.edu.cn/jzus; www.springerlink.com
E-mail: jzus@zju.edu.cn

An exact analytical solution for convective heat transfer in rectangular ducts*

Mohammad Mohsen SHAHMARDAN, Mahmood NOROUZI†‡,
Mohammad Hassan KAYHANI, Amin AMIRI DELOUEI
(*Department of Mechanical Engineering, Shahrood University of Technology, Shahrood, Iran*)
†E-mail: norouzi.mahmood@gmail.com

Received May 2, 2011; Revision accepted Aug. 11, 2011; Crosschecked Sept. 18, 2012

Abstract: An exact analytical solution is obtained for convective heat transfer in straight ducts with rectangular cross-sections for the first time. This solution is valid for both H1 and H2 boundary conditions, which are related to fully developed convective heat transfer under constant heat flux at the duct walls. The separation of variables method and various other mathematical techniques are used to find the closed form of the temperature distribution. The local and mean Nusselt numbers are also obtained as functions of the aspect ratio. A new physical constraint is presented to solve the Neumann problem in non-dimensional analysis for the H2 boundary conditions. This is one of the major innovations of the current study. The analytical results indicate a singularity occurs at a critical aspect ratio of 2.4912 when calculating the local and mean Nusselt numbers.

Key words: Exact analytical solution, Convective heat transfer, Straight duct, Rectangular cross-section, Constant heat flux
doi:10.1631/jzus.A1100122 **Document code:** A **CLC number:** TK123; O35

1 Introduction

In mechanical and chemical engineering, it is important to determine the heat transfer of fluid flow in various geometries. Such calculations are used directly in a wide range of industrial purposes such as synthesizing, designing, and optimizing the performance of various processes and systems. For example, evaluating forced convective heat transfer in closed channels is important when designing systems such as pipe lines, heat exchangers, and isolators. Consequently, many studies have employed analytical, numerical, and experimental approaches to evaluate the effect of different cross-sectional shapes, flow regions, fluid types, and thermal boundary conditions on forced convective heat transfer.

Previous studies of heat transfer in non-circular ducts have been mostly limited to numerical analysis. Fully developed laminar Newtonian flows in straight channels are generally rectilinear. Their flow fields are defined based only on the main flow velocity because secondary motions are negligible due to the dominance of viscous forces in laminar flows. Many numerical studies have investigated rectilinear convective heat transfer in closed channels. It is important to mention that H1, H2 and *T* boundary conditions refer to circumferentially constant wall temperature and axially constant wall heat flux, uniform wall heat flux both axially and circumferentially, and uniform wall temperature both axially and circumferentially, respectively. Shah and London (1978) first studied laminar forced convective heat transfer in straight and curved ducts. They used the finite difference method to obtain numerical solutions for fully developed conditions. They also developed formulations for the concept of thermally fully developed conditions for both constant heat flux and wall

‡ Corresponding author
* Project supported by the Shahrood University of Technology (No. 17024), Iran

temperature boundary conditions. Shah (1975) investigated the effect of the cross-sectional shape on forced convective heat transfer inside straight ducts, considering isosceles triangular, rounded corner equilateral triangular, sine, rhombic, and trapezoidal cross-sections using least squares matching. He found that rounding the corners of the cross-section slightly increases the heat transfer rate. Lyczkowski *et al*. (1982) and Montgomery and Wibulswas (1996) used the explicit finite difference method to investigate the Newtonian rectilinear forced convective heat transfer in the entry region of rectangular ducts. Since they ignored axial conduction in their calculations, they did not need to apply thermally fully developed conditions at the outlet, thereby simplifying the boundary conditions.

Fully developed turbulent Newtonian and laminar viscoelastic flows in non-circular channels are not rectilinear. Consequently, secondary flows may be generated in these flows. Such secondary flows appear as a pair of counter-rotating vortices near each corner of the cross-section. These vortices are considered to originate from the imbalance between the normal components of the Reynolds stresses in turbulent Newtonian flows and the second normal stress difference in viscoelastic flows. These vortices can be modeled numerically or the perturbation method can be used to investigate them analytically. Porter (1971) studied the general problem of convective heat transfer in a non-Newtonian fluid flow in straight channels. Norouzi *et al.* (2009) investigated the effect of corner vortices on mixed and forced convective heat transfer of viscoelastic flows in straight rectangular ducts. They found that corner vortices increase the flow mixing and the heat and mass transfer rates.

Zhang and Ebadian (1991) obtained an analytical/numerical solution for convective heat transfer in the thermal entrance region of ducts with various cross-sections. This solution is valid for thermally developing and hydrodynamically fully developed laminar flow. Barletta *et al.* (2003) derived a numerical solution for mixed convection in a vertical rectangular duct with H2 boundary conditions. They solved the local momentum and energy balance equations in a dimensionless form by the Galerkin finite element method and showed that the aspect ratio and the ratio of the Grashof number to the Reynolds number significantly affected the heat transfer rate. Nonino *et al.* (2006) obtained a parametric numerical solution and used it to investigate the effect of the temperature dependence of the viscosity on the simultaneously developing laminar flow of a liquid in straight ducts. They showed that the temperature dependence of the viscosity cannot be neglected under constant wall temperature boundary conditions. Furthermore, Cheng (2006) and Rennie and Vijaya Raghavan (2007) investigated the effects of the temperature dependence of the viscosity on heat transfer in a horizontal cylinder with an elliptical cross-section and a double-pipe helical exchanger, respectively. Iacovides *et al.* (2003) experimentally and numerically investigated flow and heat transfer in straight ducts with square cross-sections and with ribs along two opposite walls. They found that the ribs greatly affect fully developed flow and heat transfer. In addition, similar studies have investigated heat transfer in rectangular ducts with ribs along the walls (Jaurker *et al.*, 2006; Chang *et al.*, 2007; Saha, 2010). Sayed-Ahmed and Kishk (2008) used the finite difference method to investigate laminar flow and heat transfer of Herschel-Bulkley non-Newtonian fluids in the entrance region of a rectangular duct. They considered two thermal boundary conditions (*T* and H2) and the effects of the aspect ratio, the Prandtl number, velocity, and pressure on the temperature and the Nusselt number.

Ray and Misra (2010) analyzed the thermal characteristics of fully developed laminar flow through ducts with square and triangular cross-sections with rounded corners for H1 and H2 boundary conditions. They found that H1 boundary conditions always give a higher Nusselt number than H2 boundary conditions. Zhang and Chen (2011) investigated fluid flow and convective heat transfer in a cross-corrugated triangular duct under uniform heat flux boundary conditions using the low Reynolds number k-ε model. They showed that these channels have a higher heat transfer than conventional parallel-plate ducts. Sakalis *et al.* (2002) studied developing and fully developed flow and heat transfer in straight elliptical ducts when the duct wall temperature was kept constant, and the numerical results indicated that the friction factor decreases with decreasing aspect ratio.

Many studies have investigated flow and heat transfer in curved ducts with various cross-sections (Chen *et al.*, 2003; 2004; Ma *et al.*, 2005; 2006; Zhang *et al.*, 2007; Shen *et al.*, 2008). Rosaguti *et al.* (2007) developed a new methodology for studying

laminar flow and heat transfer behavior in periodic non-straight passages using the Newton iteration. They considered H1 thermal boundary conditions in which both the axial heat flux and the peripheral temperature are constant. Kurnia *et al.* (2011) investigated the heat transfer performance of coiled non-circular ducts and compared straight and coiled ducts. They investigated three configurations (conical, helical, and in-plane spiral) and employed a figure of merit to compare their heat transfer performances with those of a straight duct. They found that coiled ducts have higher heat transfer rates but a greater pressure drop. They also showed that a coiled duct is preferable when operating in spacious conditions and when the pumping power is not constrained. Ko and Ting (2006) and Jarungthammachote (2010) investigated entropy generation in laminar forced convection in ducts. Several studies have investigated heat transfer and entropy generation for forced convection in porous-saturated ducts with rectangular cross-sections for a constant wall temperature and a uniform wall heat flux (H1) (Haji-Sheikh *et al.*, 2006; Hooman and Haji-Sheikh, 2007; Hooman *et al.*, 2007; Hooman, 2008; 2009). Bahrami *et al.* (2009) proposed an approximate model for determining the pressure drop for fully developed slip flow through microchannels with various cross-sections. They investigated how the geometrical parameters of the microchannels affected the pressure drop.

The present paper develops an exact analytical solution for laminar fully developed convective heat transfer in straight rectangular ducts. Solutions are obtained for both H1 and H2 boundary conditions for convective heat transfer with constant heat flux at the walls. Fig. 1 depicts the geometry of the problem and the thermal boundary conditions used in this study where a and b are the half lengths of the cross-sections in the Y and Z directions, respectively and T represents the temperature, and q'' and T_w are the heat flux and wall temperature, respectively. Due to the symmetry of this problem, this study considers only one quarter of the cross-section. Exact solutions are obtained for H1 and H2 boundary conditions using the separation of variables method and various other mathematical techniques. The local and mean Nusselt numbers are also obtained for various aspect ratios from the exact solution of the temperature distributions.

The main contribution of the present study is the derivation of exact analytical solutions for H1 and H2 boundary conditions for rectangular ducts. Most previous studies of heat transfer in non-circular ducts give only numerical solutions. Analytical solutions are definitely more valuable than numerical solutions, but unfortunately it is very difficult or impossible to derive analytical solutions for complex fluids and geometries, unstable or unsteady phenomena, chaotic or turbulent flows, etc. Consequently, most previous studies have been based on numerical techniques for more realistic problems. Since the exact analytical solutions are reliable, they will be useful for validating numerical and experimental results in future studies. To the best of our knowledge, no exact analytical solution has been reported for convective heat transfer in rectangular ducts. A further innovation of the present study is that we introduce a new physical constraint for solving the Neumann problem in the non-dimensional analysis for H2 boundary conditions.

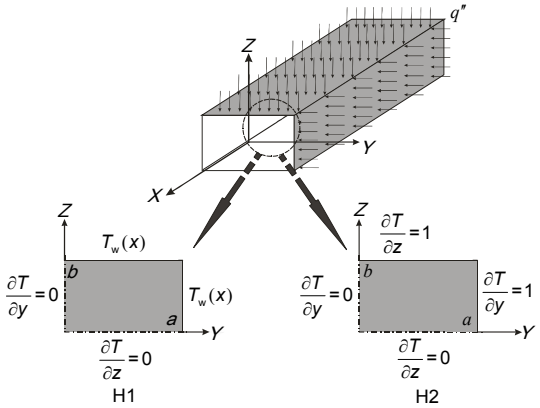

Fig. 1 Geometry and dimensionless thermal boundary conditions of channel

2 Dimensionless parameters and governing equation

We investigate analytically steady forced convective heat transfer in a straight duct with a rectangular cross-section. The continuity, momentum and energy equations for fully developed convective heat transfer in an incompressible fluid flow are as follows (Kays *et al.*, 2005):

$$\rho\frac{D\vec{\tilde{V}}}{D\tilde{t}}=-\nabla\vec{\tilde{p}}+\rho\vec{\tilde{g}}+\mu\nabla^2\vec{\tilde{V}}, \tag{1a}$$

$$\rho c_{\mathrm{p}}\tilde{V}\nabla\tilde{T}=k\nabla^2\tilde{T}, \tag{1b}$$

where ρ, c_{p}, μ, and k are the density, specific heat capacity at constant pressure, dynamic viscosity, and thermal conductivity coefficient of the fluid, respectively; $\tilde{\boldsymbol{V}}$, $\tilde{p}$, and $\tilde{T}$ are the velocity, pressure, and temperature of the fluid flow, respectively; and $\tilde{t}$ represents time. We consider fully developed laminar flow and steady-state heat transfer under a constant heat flux and assuming that the physical properties remain constant. To solve this problem, we employ dimensionless analysis using the following non-dimensional parameters:

$$\begin{aligned}&y=\frac{\tilde{y}}{d_{\mathrm{h}}},\ z=\frac{\tilde{z}}{d_{\mathrm{h}}},\ a=\frac{\tilde{a}}{d_{\mathrm{h}}},\ b=\frac{\tilde{b}}{d_{\mathrm{h}}},\\&u=\frac{\tilde{u}}{u_{\mathrm{b}}},\ \alpha=\frac{k}{\rho c_{\mathrm{p}}},\ T=q''D_{\mathrm{h}}\frac{\tilde{T}-\tilde{T}_{\mathrm{m}}}{q''D_{\mathrm{h}}/k},\end{aligned} \tag{2}$$

where y and z are coordinates in a Cartesian coordinate system, $2\tilde{a}$ and $2\tilde{b}$ are the cross-section dimensions, α is the thermal diffusivity coefficient, and $\tilde{u}$ is the main flow velocity of the fluid flow. In addition, d_{h} is the hydraulic diameter, u_{b} is the bulk velocity, and $\tilde{T}_{\mathrm{m}}$ is the mean temperature of fluid flow. These parameters are defined as follows:

$$d_{\mathrm{h}}=\frac{4\tilde{A}}{\tilde{\Gamma}}, \tag{3a}$$

$$u_{\mathrm{b}}=\frac{1}{\tilde{A}}\int_A\tilde{u}\mathrm{d}\tilde{A}, \tag{3b}$$

$$\tilde{T}_{\mathrm{m}}=\frac{1}{\rho c_{\mathrm{p}}u_{\mathrm{b}}\tilde{A}}\int_A\rho c_{\mathrm{p}}\tilde{u}\tilde{T}\mathrm{d}\tilde{A}, \tag{3c}$$

where $\tilde{A}$ and $\tilde{\Gamma}$ are the cross-sectional area and perimeter of the duct, respectively. Applying thermal energy balance to a differential control volume in the axial direction gives (Kays *et al.*, 2005):

$$q''\tilde{\Gamma}\mathrm{d}\tilde{x}=\rho\tilde{A}u_{\mathrm{b}}c_{\mathrm{p}}\mathrm{d}\tilde{T}_{\mathrm{m}}\Rightarrow\frac{\mathrm{d}\tilde{T}_{\mathrm{m}}}{\mathrm{d}\tilde{x}}=\frac{q''\tilde{\Gamma}}{\rho\tilde{A}u_{\mathrm{b}}c_{\mathrm{p}}}=\text{cte}. \tag{4}$$

To satisfy fully developed thermal conditions, Eq. (4) becomes:

$$\frac{\partial}{\partial\tilde{x}}\left(\frac{\tilde{T}-\tilde{T}_{\mathrm{m}}}{q''d_{\mathrm{h}}/k}\right)=0\Rightarrow\frac{\partial\tilde{T}}{\partial\tilde{x}}=\frac{\mathrm{d}\tilde{T}_{\mathrm{m}}}{\mathrm{d}\tilde{x}}. \tag{5}$$

Using Eqs. (4) and (5), and constant heat flux at the walls $(q''=h(\tilde{T}_{\mathrm{w}}-\tilde{T}_{\mathrm{m}}))$, we have

$$\frac{\mathrm{d}\tilde{T}}{\mathrm{d}\tilde{x}}=\frac{\partial\tilde{T}_{\mathrm{m}}}{\partial\tilde{x}}=\frac{\mathrm{d}\tilde{T}_{\mathrm{w}}}{\mathrm{d}\tilde{x}}=\frac{q''\tilde{\Gamma}}{\rho\tilde{A}u_{\mathrm{b}}c_{\mathrm{p}}}=\text{cte}. \tag{6}$$

Substituting Eqs. (2) and (6) into Eq. (1b) and setting the transverse velocity components to zero (since we are considering fully developed rectilinear flow), we obtain the following dimensionless form of the heat transfer equation:

$$\frac{\partial^2T}{\partial y^2}+\frac{\partial^2T}{\partial z^2}=4u(y,z). \tag{7}$$

Using Eq. (1a), the main velocity of rectilinear flow in a duct with a rectangular cross-section is as follows (White, 1991):

$$\begin{aligned}\tilde{u}(\tilde{y},\tilde{z})=&\frac{16\tilde{a}^2}{\mu\pi^3}\left(-\frac{\mathrm{d}\tilde{p}}{\mathrm{d}\tilde{x}}\right)\times\\&\sum_{n=1,3,5,\ldots}^{\infty}(-1)^{\frac{n-1}{2}}\left[1-\frac{\cosh\left(\frac{n\pi\tilde{z}}{2\tilde{a}}\right)}{\cosh\left(\frac{n\pi\tilde{b}}{2\tilde{a}}\right)}\right]\frac{\cos\left(\frac{n\pi\tilde{y}}{2\tilde{a}}\right)}{n^3}.\end{aligned} \tag{8a}$$

Here, u is the dimensionless main flow velocity, which is obtained using Eqs. (2) and (3b):

$$\begin{aligned}u(y,z)=&\frac{\pi}{2\kappa}\times\\&\sum_{n=1,3,5,\ldots}^{\infty}(-1)^{\frac{n-1}{2}}\left[1-\frac{\cosh\left(\frac{n\pi z}{2a}\right)}{\cosh\left(\frac{n\pi b}{2a}\right)}\right]\frac{\cos\left(\frac{n\pi y}{2a}\right)}{n^3},\end{aligned} \tag{8b}$$

where κ is a constant given by

$$\kappa=\sum_{n=1,3,5,\ldots}^{\infty}\frac{1}{n^4}\left[1-\frac{2a}{n\pi b}\mathrm{tgh}\left(\frac{n\pi b}{2a}\right)\right]. \tag{9}$$

According to Fig. 1, the thermal boundary conditions for a quarter of the cross-section (which we consider due to the symmetry of the problem) are

$$\text{for } \tilde{y}=0,\ \frac{\partial \tilde{T}}{\partial \tilde{y}}=0, \tag{10a}$$

$$\text{for } \tilde{y}=\tilde{a},\ k\frac{\partial \tilde{T}}{\partial \tilde{y}}=q'', \tag{10b}$$

$$\text{for } \tilde{z}=0,\ \frac{\partial \tilde{T}}{\partial \tilde{z}}=0, \tag{10c}$$

$$\text{for } \tilde{z}=\tilde{b},\ k\frac{\partial \tilde{T}}{\partial \tilde{z}}=q''. \tag{10d}$$

According to Eq. (2), the dimensionless form of Eq. (10) is

$$\text{for } y=0,\ \frac{\partial T}{\partial y}=0, \tag{11a}$$

$$\text{for } y=a,\ \frac{\partial T}{\partial y}=1, \tag{11b}$$

$$\text{for } z=0,\ \frac{\partial T}{\partial z}=0, \tag{11c}$$

$$\text{for } z=b,\ \frac{\partial T}{\partial z}=1. \tag{11d}$$

3 Exact solutions

3.1 Peripherally constant surface temperature

According to Eq. (11), the physical boundary conditions for constant heat flux at walls consist of a pair of homogenous and non-homogenous Neumann conditions. However, it is not possible to determine a unique solution for any differential equation using only the Neumann conditions. The prescribed wall temperature (as a Dirichlet condition) for a constant heat flux boundary condition can be used to solve the Neumann problem when solving the governing equation. By this method, the wall temperature is usually assumed to be constant in any cross-section, but is assumed to vary between different cross-sections. This assumption is exactly valid for axisymmetric problems such as convective heat transfer in straight circular or annular pipes, which have concentric isothermal lines in cross-section. However, for non-axisymmetric flows (e.g., flows in non-circular straight ducts, and in curved or coiled pipes/ducts), this assumption causes errors when calculating the temperature distribution for convective heat transfer under constant heat flux at the walls.

In this section, we present an exact solution based on this assumption, which we refer to as the H1 solution. In the next section, we obtain the other exact solution without any simplification, which we refer to as the H2 solution.

To find the H1 solution, the wall temperature is assumed to be constant and the relation $T=T_w$=cte is used instead of Eqs. (11b) and (11d). Here, we define the parameter $\theta=T-T_w$ to homogenize the boundary conditions. Therefore, the governing equation and the boundary conditions for the H1 case are given by

$$\frac{\partial^2\theta}{\partial y^2}+\frac{\partial^2\theta}{\partial z^2}=4u(y,z), \tag{12a}$$

$$\text{for } y=0,\ \frac{\partial \theta}{\partial y}=0, \tag{12b}$$

$$\text{for } y=a,\ \theta=0, \tag{12c}$$

$$\text{for } z=0,\ \frac{\partial \theta}{\partial z}=0, \tag{12d}$$

$$\text{for } z=b,\ \theta=0. \tag{12e}$$

Here, Eq. (12a) is solved using separation of variables (Myint-U and Debnath, 2007):

$$\theta(y,z)=Y(y)Z(z). \tag{13a}$$

By substituting Eq. (13a) into the homogenous form of Eq. (12a), we have

$$\frac{\mathrm{d}^2Y}{\mathrm{d}y^2}=-\frac{\mathrm{d}^2Z}{\mathrm{d}z^2}=-\lambda_n^2, \tag{13b}$$

where λ_n is the eigenvalue of the problem.

The following ordinary differential equations are obtained from Eq. (13b):

$$Y''(y)+\lambda_n^2Y(y)=0, \tag{14a}$$

$$Z''(z)-\lambda_n^2Z(z)=0. \tag{14b}$$

According to Eqs. (12b)–(12e), the boundary conditions of Eqs. (14a) and (14b) can be expressed as follows:

$$Y'(0)=0 \text{ and } Y(a)=0, \tag{15a}$$

$$Z'(0)=0 \text{ and } Z(b)=0. \tag{15b}$$

The solution of Eq. (14a) for the boundary conditions given by Eq. (15a) is

$$Y(y)=C\cos\left(\frac{n\pi y}{2a}\right),\ n=1,3,5,... \tag{16}$$

where C is an arbitrary constant coefficient. This relation introduces the eigenfunction $\theta(y,z)$ that has eigenvalues equal to $\lambda_n=n\pi/(2a)$, where n is a positive odd number. Therefore, the general solution of Eq. (12a) is

$$\theta(y,z)=\sum_{n=1,3,5,...}^{\infty} Z_n(z)\cos\left(\frac{n\pi y}{2a}\right). \tag{17}$$

Substituting the above relation into Eq. (12a) gives the following ordinary differential equation:

$$Z_n''(z)-\left(\frac{n\pi}{2a}\right)^2 Z_n(z)=\frac{2\pi}{\kappa n^3}(-1)^{\frac{n-1}{2}}\left[1-\frac{\cosh\left(\frac{n\pi z}{2a}\right)}{\cosh\left(\frac{n\pi b}{2a}\right)}\right]. \tag{18}$$

The solution of the above equation for the boundary conditions given by Eq. (15b) is

$$\begin{aligned}Z_n(z)=&\frac{\pi(-1)^{\frac{n-1}{2}}}{4\kappa n^3\lambda_n^2\cosh(\lambda_n b)}\\&\times\left\{1+2\lambda_n z+\frac{1}{e^{2\lambda_n b}+1}\left(1+\left(4\lambda_n b-3\right)e^{2\lambda_n b}\right.\right.\\&\left.-4\lambda_n b+16\cosh(\lambda_n b)e^{\lambda_n b}\right)e^{-\lambda_n z}\\&\left.+\left(1-4\cosh(\lambda_n b)\right)\left(1+e^{\lambda_n z}\right)-2\lambda_n z e^{2\lambda_n z}\right\}.\end{aligned} \tag{19}$$

By substituting Eq. (19) into Eq. (17), the temperature distribution for the H1 boundary conditions is obtained:

$$\begin{aligned}\theta(y,z)=&\sum_{n=1,3,5,...}^{\infty}\frac{\pi(-1)^{\frac{n-1}{2}}}{4\kappa n^3\lambda_n^2\cosh(\lambda_n b)}\times\left\{1+2\lambda_n z\right.\\&+\frac{e^{-\lambda_n z}}{(e^{2\lambda_n b}+1)}\left(1+(4\lambda_n b-3)e^{2\lambda_n b}-4\lambda_n b+16\cosh(\lambda_n b)e^{\lambda_n b}\right)\\&\left.+\left(1-4\cosh(\lambda_n b)\right)(1+e^{\lambda_n z})-2\lambda_n z e^{2\lambda_n z}\right\}\cos(\lambda_n y).\end{aligned} \tag{20}$$

The convection coefficient can be found using the following relation:

$$h=\frac{q''}{\tilde{T}_w-\tilde{T}_m}=\frac{q''}{-\tilde{\theta}_m}. \tag{21}$$

Therefore, the Nusselt number for H1 boundary conditions is calculated using the following relation:

$$Nu=-\frac{1}{\theta_m}=-\frac{1}{\frac{1}{u_b A}\int_A u\theta\mathrm{d}A}. \tag{22}$$

3.2 Peripherally constant heat flux

As mentioned above, the H2 solution refers to the solution of convective heat transfer of fluid flow for a constant heat flux obtained without making any simplifying assumptions about the wall temperature. The Neumann condition ensures that it is not possible to find a unique solution for this problem due to the temperature distribution having an unknown constant. This constant can be determined by applying a physical constraint such as the temperature at one point on the wall or in the flow field (Shah, 1975). Here, we employ another physical constraint that is suitable for solving the non-dimensional form of the heat transfer equation. By taking the product of the main flow velocity ($u(y,z)$) and the non-dimensional temperature (Eq. (2)), and integrating it over the cross-section, we can obtain

$$\int_A uT\mathrm{d}A=0. \tag{23}$$

All the parameters in the above constraint are dimensionless. This physical constraint represents the main innovation of the current investigation. It could be generalized to convective heat transfer for fluid

flow in other closed channels, such as curved and coiled ducts, fin tubes, and ribbed channels.

To find the H2 solution for the energy equation (Eq. (7)), it is necessary to homogenize the relevant boundary conditions (Eq. (11)). Consequently, the parameter θ should be defined as follows:

$$\theta(y,z)=T(y,z)-\frac{y^2}{2a}-\frac{z^2}{2b}. \tag{24}$$

By substituting the above equation into Eqs. (7) and (11), the following partial differential equation and homogeneous boundary conditions are obtained:

$$\frac{\partial^2\theta}{\partial y^2}+\frac{\partial^2\theta}{\partial z^2}=4(u-1), \tag{25a}$$

$$\text{for } y=0,\ \frac{\partial\theta}{\partial y}=0, \tag{25b}$$

$$\text{for } y=a,\ \frac{\partial\theta}{\partial y}=0, \tag{25c}$$

$$\text{for } z=0,\ \frac{\partial\theta}{\partial z}=0, \tag{25d}$$

$$\text{for } z=b,\ \frac{\partial\theta}{\partial z}=0. \tag{25e}$$

To solve Eq. (25a), it is necessary to find the eigenfunction of this problem. It can be determined by solving the homogeneous form of Eq. (25a) (Myint-U and Debnath, 2007). Therefore, by substituting the separated-variable form of the solution ($\theta(y,z)=Y(y)Z(z)$) into the homogeneous form of Eq. (25a) (Laplace equation), we have

$$Y''(y)+\lambda^2Y(y)=0, \tag{26a}$$

$$Z''(z)-\lambda^2Z(z)=0. \tag{26b}$$

According to Eqs. (25b)–(25e), the boundary conditions of Eqs. (26a) and (26b) should be

$$Y'(0)=0 \text{ and } Y'(a)=0, \tag{27a}$$

$$Z'(0)=0 \text{ and } Z'(b)=0. \tag{27a}$$

Solving Eq. (26a) by applying the boundary conditions given in Eq. (27a), the eigenfunction for this problem is obtained as follows:

$$Y_m=\cos\left(\frac{m\pi}{L}\right),\ m=0,1,2,... \tag{28}$$

Therefore, the solution of Eq. (25a) should be

$$\theta(y,z)=Z_0(z)+\sum_{m=1,2,...}^{\infty}Z_m(z)\cos\left(\frac{m\pi y}{a}\right). \tag{29}$$

Substituting Eq. (29) into Eq. (25a) gives the following ordinary differential equation for $Z(z)$:

$$Z_0''(z)+\sum_{m=1,2,...}^{\infty}\left[Z_m''(z)-\left(\frac{m\pi}{a}\right)^2Z_m(z)\right]\times\cos\left(\frac{m\pi y}{a}\right)=4(u(y,z)-1). \tag{30}$$

From the Fourier series expansion, we obtain the following relation for the zeroth-order term of this series:

$$Z_0''=\frac{1}{a}\int_0^a\left[4\left(u(y,z)-1\right)\right]\mathrm{d}y. \tag{31}$$

Integrating this expression twice, we obtain

$$Z_0=\frac{4}{\kappa}\sum_{n=1,3,5,...}^{\infty}\frac{1}{n^4}\left[\frac{z^2}{2}-\left(\frac{2a}{n\pi}\right)^2\frac{\cosh\left(\frac{n\pi z}{2a}\right)}{\cosh\left(\frac{n\pi b}{2a}\right)}\right]-2z^2+c_1z+c_2. \tag{32}$$

The factor $\left[Z_m''(z)-(m\pi/a)^2Z_m(z)\right]$ in Eq. (30) is the cosine coefficient of the Fourier series. It can be obtained from the following equation:

$$\begin{aligned}&Z_m''(z)-\left(\frac{m\pi}{a}\right)^2Z_m(z)\\&=\frac{2}{a}\int_0^a\left[4\left(u(y,z)-1\right)\right]\cos\left(\frac{m\pi y}{a}\right)\mathrm{d}y\\&=\frac{4}{\kappa}\sum_{n=1,3,5,...}^{\infty}\frac{1}{n^3}\gamma_{nm}\left[1-\frac{\cosh\left(\frac{n\pi z}{2a}\right)}{\cosh\left(\frac{n\pi b}{2a}\right)}\right],\end{aligned} \tag{33}$$

where γ_{nm} is

$$\gamma_{nm}=\frac{(-1)^{n+m-1}}{n+2m}+\frac{(-1)^{n-m-1}}{n-2m}. \tag{34}$$

The particular solution of Eq. (33) is

$$Z_{m_p}=\sum_{n=1,3,5,\ldots}^{\infty}\left[a_n+b_n\cosh\left(\frac{n\pi z}{2a}\right)\right]. \tag{35}$$

Substituting this solution into Eq. (33) yields the coefficients a_n and b_n:

$$a_n=\frac{4}{\kappa n^3}\frac{-1}{\left(\frac{m\pi}{a}\right)^2}\gamma_{nm}, \tag{36a}$$

$$b_n=\frac{4}{\kappa n^3}\frac{-1}{\left[\left(\frac{n\pi}{2a}\right)^2-\left(\frac{m\pi}{a}\right)^2\right]}\frac{1}{\cosh\left(\frac{n\pi b}{2a}\right)}\gamma_{nm}. \tag{36b}$$

The homogenous solution of Eq. (33) is given by

$$Z_{m_h}=c_m\sinh\left(\frac{m\pi z}{a}\right)+d_m\cosh\left(\frac{m\pi z}{a}\right), \tag{37}$$

where c_m and d_m are unknown coefficients. Finally, the main solution, $Z_m(z)$ is

$$Z_m(z)=Z_{m_h}(z)+Z_{m_p}(z). \tag{38}$$

The term $\theta(y,z)$ is obtained by substituting Eqs. (32) and (38) into Eq. (29). To determine the remaining constants, the boundary conditions in the z direction (Eqs. (25d) and (25e)) are applied to the modified temperature distribution ($\theta(y,z)$):

$$c_1+\sum_{m=1,2,\ldots}^{\infty}c_m\left(\frac{m\pi}{a}\right)\cos\left(\frac{m\pi y}{a}\right)=0\Rightarrow c_1=c_m=0, \tag{39a}$$

$$\sum_{m=1,2,\ldots}^{\infty}\left[d_m\left(\frac{m\pi}{a}\right)\sinh\left(\frac{m\pi b}{a}\right)+\sum_{n=1,3,\ldots}^{\infty}b_n\left(\frac{n\pi}{2a}\right)\sinh\left(\frac{n\pi b}{2a}\right)\right]\times\cos\left(\frac{m\pi y}{a}\right)=0$$

$$\Rightarrow d_m=\frac{a}{m\pi}\frac{-1}{\sinh\left(\frac{m\pi b}{a}\right)}\sum_{n=1,3,\ldots}^{\infty}b_n\left(\frac{n\pi}{2a}\right)\sinh\left(\frac{n\pi b}{2a}\right). \tag{39b}$$

Finally, $T(y,z)$ is obtained using $\theta(y,z)$ and Eq. (24):

$$\begin{aligned}T(y,z)=&c_2+\frac{y^2}{2a}+\frac{z^2}{2b}-2z^2\\&+\frac{4}{\kappa}\sum_{n=1,3,5,\ldots}^{\infty}\frac{1}{n^4}\left[\frac{z^2}{2}-\left(\frac{2a}{n\pi}\right)^2\frac{\cosh\left(\frac{n\pi z}{2a}\right)}{\cosh\left(\frac{n\pi b}{2a}\right)}\right]\\&+\sum_{m=1,2,\ldots}^{\infty}\left[d_m\cosh\left(\frac{m\pi z}{a}\right)+\sum_{n=1,3,5,\ldots}^{\infty}\left[a_n+b_n\cosh\left(\frac{n\pi z}{2a}\right)\right]\right]\cos\left(\frac{m\pi y}{a}\right),\end{aligned} \tag{40}$$

where c_2 is the only unknown constant and can be obtained by applying a physical constraint (Eq. (23)). This constant is obtained by substituting Eqs. (8b) and (40) into Eq. (23), and calculating the resulting integral. It is listed in Table 1 for some typical aspect ratios. Table 1 shows that c_2 increases rapidly with increasing aspect ratio. Therefore, the dimensionless temperature distribution for the H2 boundary conditions (Eq. (40)) can be calculated from constant c_2. Here, the local convection coefficient is obtained by applying the energy balance at the walls,

$$h=\frac{k\frac{\partial\tilde{T}}{\partial\tilde{n}}}{\tilde{T}_w-\tilde{T}_m}. \tag{41}$$

The local Nusselt number is determined from Eqs. (2) and (41):

$$Nu=1/T_w. \tag{42}$$

The peripherally mean the Nusselt number is defined as the average of the local Nusselt numbers on the perimeter of the cross-section (Bejan, 2004):

$$\overline{Nu}=\frac{1}{p}\int_p Nu\mathrm{d}l, \tag{43}$$

Table 1 Values of c_2 in terms of different aspect ratios

a/b	c_2	a/b	c_2
1	0.2532	7	335.7524
1.43	1.1555	8	551.6134
2	3.8382	10	1275.0440
3	15.8311	12	2545.9509
4	43.8393	15	5978.9989
6	190.2218	30	88233.6340

where l is the length and p is the perimeter of the cross-section. The fully developed rectilinear convective heat transfer in closed straight channels is independent of the Reynolds and Prandtl numbers (Bejan, 2004; Kays *et al.*, 2005). The dimensionless solutions for the temperature distribution for both the H1 and H2 boundary conditions in the current study (Eqs. (20) and (40)) are also independent of the Reynolds and Prandtl numbers.

3.3 Checking the physical constraint for the H2 boundary conditions peripherally constant heat flux

In this section, we investigate the validity of the physical constraint for the H2 boundary conditions, which were introduced above (Eq. (23)). The H1 and H2 boundary conditions are identical for axisymmetric problems such as convective heat transfer in straight circular and annular ducts. The H1 solution of this problem is a well-known solution that has been reported in many studies. Therefore, we attempt to find other exact solutions for H2 boundary conditions based on the physical constraint Eq. (23) and compare the results with the solutions for the H1 boundary conditions.

To find an exact H2 solution for fully developed convective heat transfer in a straight circular pipe, we define the following dimensionless parameters:

$$r=\frac{\tilde{r}}{d_{\mathrm{h}}}, \tag{44a}$$

$$u=\frac{\tilde{u}}{u_{\mathrm{b}}}=2(1-4r^2). \tag{44b}$$

The dimensionless energy equation is given as

$$\frac{1}{r}\frac{\partial}{\partial r}\left(r\frac{\partial T}{\partial r}\right)=8(1-4r^2). \tag{45}$$

The H2 boundary conditions for this problem are

$$\left.\frac{\partial T}{\partial r}\right|_{r=0}=0, \tag{46a}$$

$$\left.\frac{\partial T}{\partial r}\right|_{r=0.5}=1. \tag{46b}$$

The general solution for the dimensionless temperature is obtained by solving Eq. (45):

$$T(r)=2(r^2-r^4)+c_1\ln(r)+c_2. \tag{47}$$

By applying the boundary conditions (Eq. (46a) or (46b)), c_1 is calculated to be zero while c_2 remains unknown, which is related to the Neumann problem. This term could be calculated by applying the constraint given by Eq. (23). By substituting Eqs. (44b) and (47) into Eq. (23), c_2 is found to be −7/48. Therefore, the dimensionless temperature is

$$T(r)=2(r^2-r^4)-\frac{7}{48}. \tag{48}$$

Here, the local and mean Nusselt numbers are identical and are given by

$$Nu=\frac{hd_{\mathrm{h}}}{k}=\frac{\left.\dfrac{\partial T}{\partial r}\right|_{r=0.5}}{\left.T\right|_{r=0.5}}=\frac{1}{\left.T\right|_{r=0.5}}=\frac{48}{11}\approx 4.3636. \tag{49}$$

The above Nusselt number for fully developed convective heat transfer for flow in a straight pipe under a constant heat flux at a wall was reported by Shah and London (1978), based on the H1 boundary conditions. Here, we show that a similar solution is obtained for H2 boundary conditions using the physical constraint given by Eq. (23). Therefore, we conjecture that the physical constraint given by Eq. (23) could be used to solve the Neumann problem for convective heat transfer under the H2 boundary conditions for both axisymmetric and non-axisymmetric cases.

4 Results and discussion

This section presents analytical solution results for convective heat transfer for flow in straight rectangular ducts under the H1 and H2 boundary conditions. It is first necessary to study the convergence of the series of the solutions for the H1 and H2 boundary conditions (Eqs. (20) and (40)). Fig. 2a shows the maximum variation in the non-dimensional form of the temperature for the H1 solution (Eq. (20)) for

different Fourier series indices (n). According to Eq. (20), the even terms in the series for the H1 solution are zero. Consequently, Fig. 2a shows only the odd terms ((n−1)/2). As shown in Fig. 2a, this series converges rapidly for all aspect ratios. The rate of convergence is the quickest for the square cross-section. The rate of convergence decreases when the aspect ratio is reduced below unity.

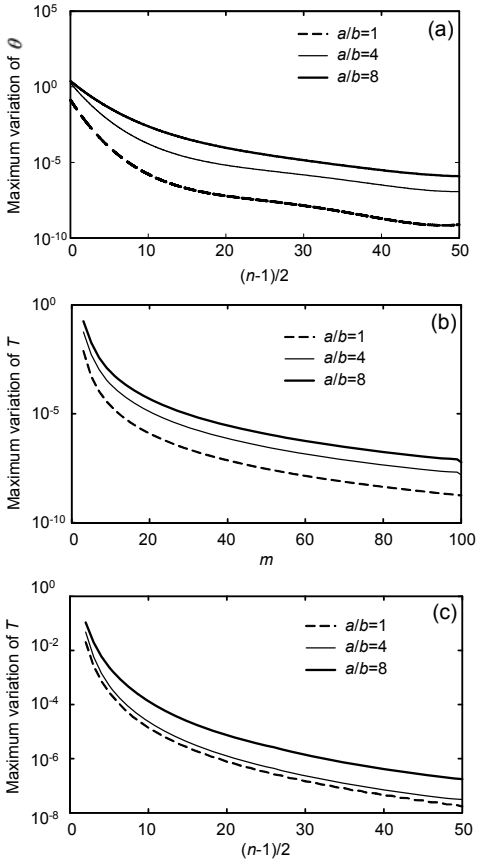

Fig. 2 Maximum variation of non-dimensional form of the temperature distribution in terms of different values of Fourier series' counters
(a) H1 solution (refer to Eq. (20)); (b) H2 solution based on the first counter (m); (c) H2 solution based on the second counter (refer to Eq. (40))

Eq. (40) shows that the dimensionless temperature for the H2 boundary conditions consists of several series with independent indices m and n. Figs. 2b and 2c shows the maximum variations in the dimensionless temperature for different values of the series indices (m and n). This figure shows that the Fourier series for the temperature distribution for the H2 boundary condition converges. To achieve convergence to within 10^{-7} for aspect ratios smaller than 1:8, it is sufficient to calculate approximately 200 terms of n for the H1 boundary conditions and 100 terms of m and n for the H2 boundary conditions.

Fig. 3 shows dimensionless contours for the temperature distribution (θ=T−T_w) for the H1 boundary conditions for some typical aspect ratios. Due to the symmetry, these contours are shown only for one quarter of the cross-section. The results are presented for the heating case, so the maximum value (zero) of θ occurs at the wall and θ is negative within the cross-section. Fig. 3 shows that if the peripheral wall temperature is assumed to be constant, the temperature distribution for the H1 boundary conditions will be similar to the main velocity distribution. While this assumption solves the Neumann problem, the results obtained deviate from the solution for the temperature distribution for non-axisymmetric flows for constant heat flux at the walls.

Fig. 4 shows temperature distributions for the H2 boundary conditions for various aspect ratios. Similar to Fig. 3, these contours are shown in one quarter of the cross-section. As mentioned above, the solution for the H2 boundary conditions is the solution for the temperature distribution of any flow for a constant heat flux. In this case, the wall temperature is not constant along the perimeter of the cross-section. Furthermore, a temperature of zero at any location implies that the temperature at that location is equal to the mean fluid flow temperature (Eq. (2) defines the dimensionless temperature). As mentioned above, the H1 and H2 solutions are identical for axisymmetric flows. Comparison of Figs. 3 and 4 reveals that the deviation between the H1 and H2 solutions becomes greater at higher aspect ratios. This is related to the greater deviation of the flow from axisymmetric flow.

Table 2 lists the Nusselt number for fully developed convective heat transfer of flow in a straight rectangular duct for the H1 boundary conditions. The Nusselt number was calculated from Eq. (22). According to Table 2, the Nusselt numbers obtained from the exact solution of present study agree reasonably with the numerical results of Shah and London (1978).

The accuracy of the physical constraint introduced in the current study for solving the H2 boundary conditions was considered in Section 3.3. The validity of our solution for the H2 boundary conditions of non-circular ducts can be checked for square

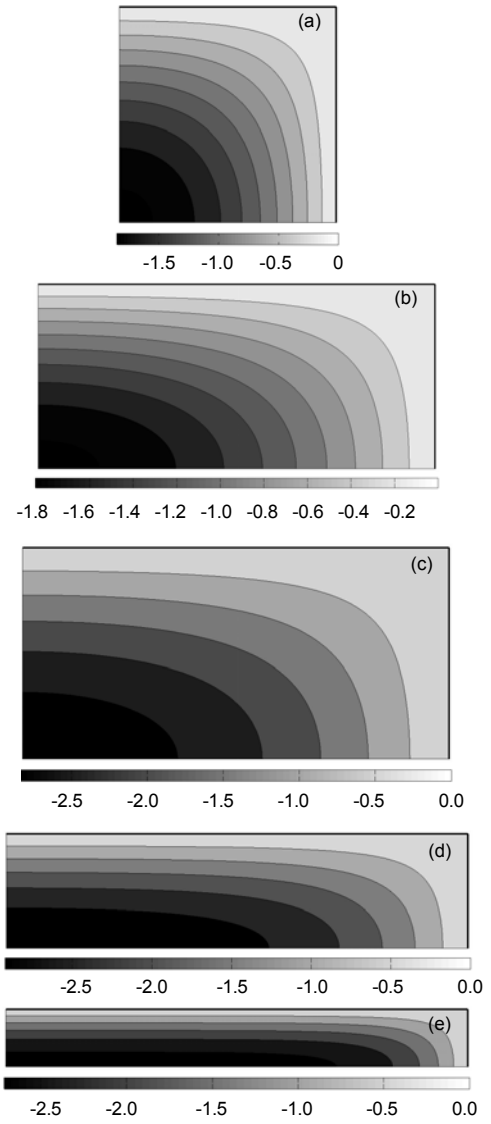

Fig. 3 Temperature distribution of H1 condition ($\theta=T-T_w$) in a one-quarter of cross-section at different aspect ratios
(a) a/b=1; (b) a/b=1.43; (c) a/b=2; (d) a/b=4; (d) a/b=8

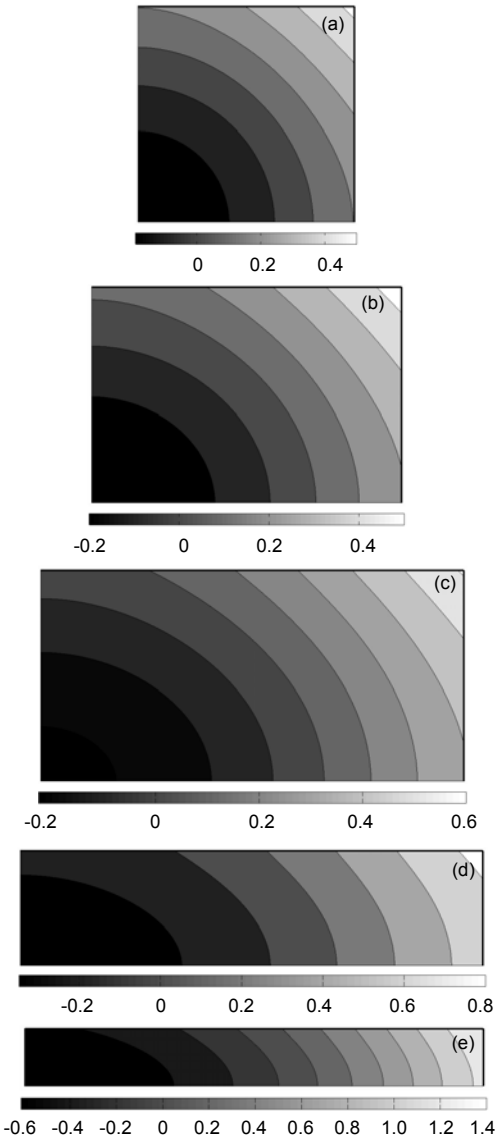

Fig. 4 Temperature distribution of H2 condition in a one-quarter of cross-section at different aspect ratios
(a) a/b=1; (b) a/b=1.43; (c) a/b=2; (d) a/b=4; (d) a/b=8

Table 2 Values of Nusselt number of H1 solution at different aspect ratios

a/b	Nu (proposed investigation)	Nu (Shah and London, 1978)
1	3.6112	3.61
1.43	3.7328	3.73
2	4.1208	4.12
3	4.7936	4.79
4	5.3341	5.33
8	6.4905	6.49

cross-sections. According to the numerical solution of Shah (1975), the mean Nusselt number for convective heat transfer in a straight square duct is 3.38, which is equal to the values given by Eqs. (40), (42), and (43) (Table 3).

To find the local Nusselt numbers for the H2 boundary conditions, the dimensionless temperature distribution on each wall should be determined. Figs. 5a and 5b show the temperature distribution at $z=b$ (upper wall of the cross-section) and $y=a$ (right-hand side of the cross-section) for various aspect ratios. According to Eq. (42), the local Nusselt number is inversely proportional to the dimensionless temperature. Therefore, a dimensionless temperature

of zero at the wall results in a singularity when calculating the local Nusselt number. As shown in Fig. 5a, the temperature is zero on the upper wall for $a/b \geq 2.4912$. According to Fig. 5b, there is no singularity for $y=a$ (smaller wall). This is clearer in Fig. 6, which shows the temperature distributions for various aspect ratios. Fig. 6 shows that there is no singularity in the local Nusselt number for aspect ratios smaller than 2.4912. Therefore, the aspect ratio of 2.4912 is a critical aspect ratio at which the temperature is zero in the middle of the wall. When the aspect ratio is increased above 2.4912, the singularity shifts to the edge of the wall (upper wall in the present study).

Table 3 Values of Nusselt number of H2 solution at different aspect ratios

a/b	Nu (exact solution)	a/b	Nu (exact solution)
1	3.38	8	−0.38
1.43	3.69	10	−0.35
2	5.30	12	−0.32
3	−0.26	15	−0.28
4	−0.37	30	−0.16

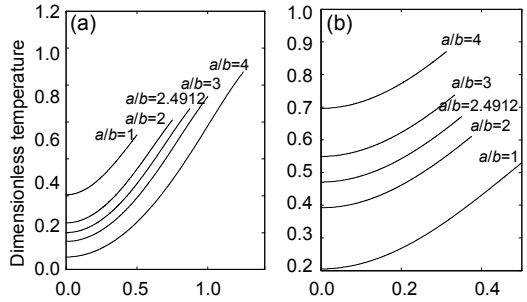

Fig. 5 Dimensionless temperature distribution at different aspect ratios on $z=b$ side (a) and $y=a$ side (b) of cross-section ($z=b$ is the larger side of cross-section)

Fortunately, despite the possibility of a singularity in the local Nusselt number, the mean peripheral Nusselt number can be uniquely determined from Eq. (43). We used MATLAB software to calculate the singular integration Eq. (43). This integration is determined by global adaptive quadrature, which is implemented in a MATLAB function (quadgk).

The mean Nusselt numbers of the top and right-hand sides of the cross-section are called Nu_y and Nu_z, respectively. Fig. 7 shows Nu_y, Nu_z, and the perimeter mean Nusselt numbers as functions of the aspect ratio. It shows that increasing the aspect ratio reduces Nu_z, which is due to the increase in the temperature on the right-hand side of the cross-section. Increasing the aspect ratio from 1 to 2.4912 causes Nu_y and the perimeter mean Nusselt number to increase quickly. Here, Nu_y and Nu tend to infinity at the critical Nusselt number. Since the local and overall heat transfer rates are constant for the H2 solution, an infinite Nusselt number does not imply that infinite heat transfer occurs. It only implies that the temperature at the middle of the upper wall is equal to the mean fluid flow temperature. When aspect ratios are greater than 2.4912, these two Nusselt numbers are negative and tend to zero. Table 3 gives the mean Nusselt numbers for the H2 boundary conditions for several typical aspect ratios.

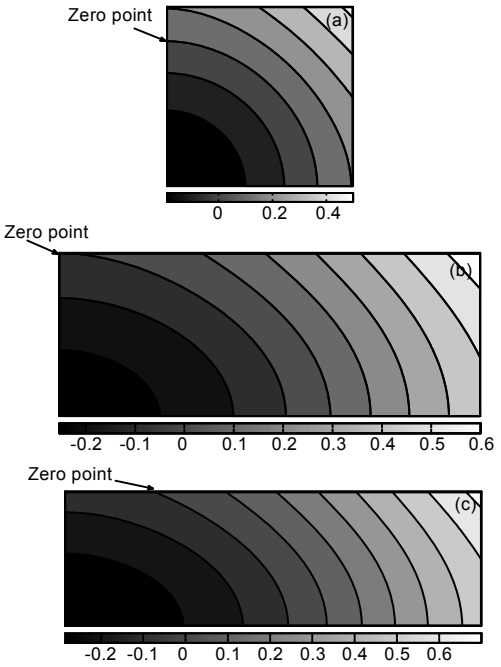

Fig. 6 Location of singularity point in different aspect ratios
(a) $a/b=2$; (b) $a/b=2.4912$; (c) $a/b=3$

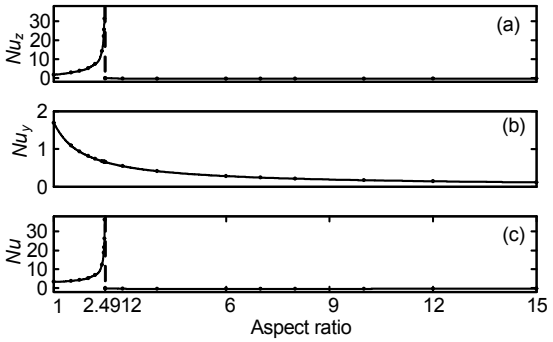

Fig. 7 Values of mean Nusselt number in terms of aspect for (a) the right-hand side, (b) top side and (c) perimeter of the cross section

5 Conclusions

An exact analytical solution for fully developed convective heat transfer in rectangular ducts under a constant heat flux was derived for the first time. Closed forms of the temperature distribution for both H1 and H2 solutions were obtained (Eqs. (20) and (40)). The main conclusions of the current study are summarized below.

1. A new physical constraint is presented for solving the Neumann problem when solving the non-dimensional form of the H2 problem (Eq. (23)). This constraint could be used to solve other fully developed problems such as convective heat transfer in non-circular ducts, elbows, and coiled tubes.

2. The analytical solution obtained reveals that the H1 and H2 solutions deviate and that this deviation increases at higher aspect ratios, which is related to the greater deviation of flow from axisymmetric flow. These two solutions are identical for axisymmetric problems. Therefore, the H1 solution is only suitable for aspect ratios close to unity (i.e., square cross-sections) because the accuracy of this solution decreases dramatically at higher aspect ratios.

3. The results show that at a critical aspect ratio of 2.4912 for the H2 solution, the temperature in the middle of the larger wall is equal to the mean fluid flow temperature. This generates a singularity when calculating the local and mean Nusselt numbers (Eqs. (42) and (43)). For aspect ratios smaller than 2.4912, the wall temperature is higher than the mean fluid flow temperature, thus no singularity occurs for either the mean or local Nusselt number. For aspect ratios larger than this critical aspect ratio, there is a singularity in the local Nusselt number in the larger side of the cross-section, but the mean peripheral Nusselt number remains unique and definite.

References

Bahrami, M., Tamayol, A., Taheri, P., 2009. Slip-flow pressure drop in microchannels of general cross section. *Journal of Fluids Engineering*, **131**(3):031201. [doi:10.1115/1.3059699]

Barletta, A., Rossi di Schio, E., Zanchini, E., 2003. Combined forced and free flow in a vertical rectangular duct with prescribed wall heat flux. *International Journal of Heat and Fluid Flow*, **24**(6):874-887. [doi:10.1016/S0142-727X(03)00090-0]

Bejan, A., 2004. Convection Heat Transfer (3rd Edition). Wiley, New York.

Chang, S.W., Yang, T.L., Huang, R.F., Sung, K.C., 2007. Influence of channel-height on heat transfer in rectangular channels with skewed ribs at different bleed conditions. *International Journal of Heat and Mass Transfer*, **50**(23-24):4581-4599. [doi:10.1016/j.ijheatmasstransfer.2007.03.033]

Chen, H.J., Zhang, B.Z., Zhang, J.S., 2003. Fluid flow in rotating helical square ducts. *Journal of Hydrodynamics Series B*, **15**(3):49-56.

Chen, H.J., Shen, X.R., Zhang, B.Z., 2004. The laminar flow and heat transfer in the developing region of helical square ducts. *Journal of Hydrodynamics Series B*, **16**(3):267-275.

Cheng, C.Y., 2006. The effect of temperature-dependent viscosity on the natural convection heat transfer from a horizontal isothermal cylinder of elliptic cross section. *International Communications in Heat and Mass Transfer*, **33**(8):1021-1028. [doi:10.1016/j.icheatmasstransfer.2006.02.019]

Haji-Sheikh, A., Nield, D.A., Hooman, K., 2006. Heat transfer in the thermal entrance region for flow through rectangular porous passages. *International Journal of Heat and Mass Transfer*, **49**(17-18):3004-3015. [doi:10.1016/j.ijheatmasstransfer.2006.01.040]

Hooman, K., 2008. A perturbation solution for forced convection in a porous-saturated duct. *Journal of Computational and Applied Mathematics*, **211**(1):57-66. [doi:10.1016/j.cam.2006.11.005]

Hooman, K., 2009. Slip flow forced convection in a microporous duct of rectangular cross-section. *Applied Thermal Engineering*, **29**(5-6):1012-1019. [doi:10.1016/j.applthermaleng.2008.05.007]

Hooman, K., Haji-Sheikh, A., 2007. Analysis of heat transfer and entropy generation for a thermally developing Brinkman-Brinkman forced convection problem in a rectangular duct with isoflux walls. *International Journal of Heat and Mass Transfer*, **50**(21-22):4180-4194. [doi:10.1016/j.ijheatmasstransfer.2007.02.036]

Hooman, K., Gurgenci, H., Merrikh, A.A., 2007. Heat transfer and entropy generation optimization of forced convection in porous-saturated ducts of rectangular cross-section. *International Journal of Heat and Mass Transfer*, **50**(11-12):2051-2059. [doi:10.1016/j.ijheatmasstransfer.2006.11.015]

Iacovides, H., Kelemenis, G., Raisee, M., 2003. Flow and heat transfer in straight cooling passages with inclined ribs on opposite walls: an experimental and computational study. *Experimental Thermal and Fluid Science*, **27**(3):283-294.

Jarungthammachote, S., 2010. Entropy generation analysis for fully developed laminar convection in hexagonal duct subjected to constant heat flux. *Energy*, **35**(12):5374-5379. [doi:10.1016/j.energy.2010.07.020]

Jaurker, A.R., Saini, J.S., Gandhi, B.K., 2006. Heat transfer and friction characteristics of rectangular solar air heater duct using rib-grooved artificial roughness. *Solar Energy*, **80**(8):895-907. [doi:10.1016/j.solener.2005.08.006]

Kays, W.M., Crawford, M.E., Weigand, B., 2005. Convective

Heat and Mass Transfer (4th Edition). McGraw-Hill, New York.

Ko, T.H., Ting, K., 2006. Entropy generation and optimal analysis for laminar forced convection in curved rectangular ducts: A numerical study. *International Journal of Thermal Sciences*, **45**(2):138-150. [doi:10.1016/j.ijthermalsci.2005.01.010]

Kurnia, J.C., Sasmito, A.P., Mujumdar, A.S., 2011. Evaluation of the heat transfer performance of helical coils of non-circular tubes. *Journal of Zhejiang University-SCIENCE A (Applied Physics & Engineering)*, **12**(1): 63-70. [doi:10.1631/jzus.A1000296]

Lyczkowski, R.W., Solbring, C.W., Gidaspow, D., 1982. Forced convection heat transfer in rectangular ducts-general case of wall resistances and peripheral conduction for ventilation cooling of nuclear waste repositories. *Nuclear Engineering and Design*, **67**(3): 357-378.

Ma, J.F., Shen, X.R., Zhang, B.Z., Chen, H.J., 2005. Numerical analysis on the fluid flow in a rotating curved elliptical pipe. *Journal of Hydrodynamics Series B*, **17**(2):171-178.

Ma, J.F., Shen, X.R., Zhang, M.K., Zhang, B.Z., 2006. Laminar developing flow in the entrance region of rotating curved pipes. *Journal of Hydrodynamics Series B*, **18**(4): 418-423.

Montgomery, S.R., Wibulswas, P., 1996. Laminar Flow Heat Transfer in Ducts of Rectangular Cross-Section. The Third International Heat Transfer Conference, New York, p.85-98.

Myint-U, T., Debnath, L., 2007. Linear Partial Differential Equations for Scientists and Engineers. Birkhauser, Boston.

Nonino, C., DelGiudice, S., Savino, S., 2006. Temperature dependent viscosity effects on laminar forced convection in the entrance region of straight ducts. *International Journal of Heat and Mass Transfer*, **49**(23-24):4469-4481. [doi:10.1016/j.ijheatmasstransfer.2006.05.02]

Norouzi, M., Kayhani, M.H., Nobari, M.R.H., 2009. Mixed and forced convection of viscoelastic materials in straight duct with rectangular cross section. *World Applied Sciences Journal*, **7**(3):285-296.

Porter, J.E., 1971. Heat transfer at low Reynolds number (highly viscous liquids in laminar flow). *Transactions of the Institution of Chemical Engineers*, **49**:1-29.

Ray, S., Misra, D., 2010. Laminar fully developed flow through square and equilateral triangular ducts with rounded corners subjected to H1 and H2 boundary conditions. *International Journal of Thermal Sciences*, **49**(9): 1763-1775. [doi:10.1016/j.ijthermalsci.2010.03.012]

Rennie, T.J., Vijaya Raghavan, G.S., 2007. Thermally dependent viscosity and non-Newtonian flow in a double-pipe helical heat exchanger. *Applied Thermal Engineering*, **27**(5-6): 862-868. [doi:10.1016/j.applthermaleng.2006.09.006]

Rosaguti, N.R., Fletcher, D.F., Haynes, B.S., 2007. A general implementation of the H1 boundary condition in CFD simulations of heat transfer in swept passages. *International Journal of Heat and Mass Transfer*, **50**(9-10): 1833-1842. [doi:10.1016/j.ijheatmasstransfer.2006.10.009]

Saha, S.K., 2010. Thermal and friction characteristics of laminar flow through rectangular and square ducts with transverse ribs and wire coil inserts. *Experimental Thermal and Fluid Science*, **34**(1):63-72. [doi:10.1016/j.expthermflusci.2009.09.003]

Sakalis, V.D., Hatzikonstantinou, P.M., Kafousias, N., 2002. Thermally developing flow in elliptic ducts with axially variable wall temperature distribution. *International Journal of Heat and Mass Transfer*, **45**(1):25-35. [doi:10.1016/S0017-9310(01)00124-7]

Sayed-Ahmed, M.E., Kishk, K.M., 2008. Heat transfer for Herschel-Bulkley fluids in the entrance region of a rectangular duct. *International Communications in Heat and Mass Transfer*, **35**(8):1007-1016. [doi:10.1016/j.icheatmasstransfer.2008.05.002]

Shah, R.K., 1975. Laminar flow friction and forced convection heat transfer in ducts of arbitrary geometry. *International Journal of Heat and Mass Transfer*, **18**(7-8):849-862. [doi:10.1016/0017-9310(75)90176-3]

Shah, R.K., London, A.L., 1978. Laminar Flow Forced Convection in Ducts. Academic Press, New York.

Shen, X.R., Zhang, M.K., Ma, J.F., Zhang, B.Z., 2008. Flow and heat transfer of oldroyd-B fluids in a rotating curved pipe. *Journal of Hydrodynamics Series B*, **20**(1):39-46. [doi:10.1016/S1001-6058(08)60025-6]

White, F.M., 1991. Viscous Fluid Flow (2nd Edition). McGraw-Hill, New York.

Zhang, H.Y., Ebadian, M.A., 1991. An analytical/numerical solution of convective heat transfer in the thermal entrance region of irregular ducts. *International Communications in Heat and Mass Transfer*, **18**(2):273-291. [doi:10.1016/0735-1933(91)90019-Z]

Zhang, L.Z., Chen, Z.Y., 2011. Convective heat transfer in cross-corrugated triangular ducts under uniform heat flux boundary conditions. *International Journal of Heat and Mass Transfer*, **54**(1-3):597-605. [doi:10.1016/j.ijheatmasstransfer.2010.09.010]

Zhang, M.K., Shen, X.R., Ma, J.F., Zhang, B.Z., 2007. Flow of oldroyd-B fluid in rotating curved square ducts. *Journal of Hydrodynamics Series B*, **19**(1):36-41. [doi:10.1016/S1001-6058(07)60025-0]